ARTICLE NO. 79-0273R

J80-028

0001
0017
30003

The Supersonic Triplet—A New Aerodynamic Panel Singularity with Directional Properties

Frank A. Woodward*
Analytical Methods, Inc., Bellevue, Wash.
and
Emma Jean Landrum†
NASA Langley Research Center, Hampton, Va.

A new supersonic triplet singularity has been developed which eliminates internal waves generated by a panel having supersonic edges. The triplet is a linear combination of source and vortex distributions which provides the desired directional properties in the flowfield surrounding the panel. The theoretical development of the triplet is described, together with its application to the calculation of surface pressure on arbitrary body shapes. Examples are presented comparing the results of the new method with other supersonic panel methods and with experimental data.

Nomenclature

a	= panel inclination
b	= panel leading-edge span
c	= panel chord
C	= attenuation factor
d	= hyperbolic distance to panel corner
D	= hyperbolic distance to panel apex
F,G,H	= velocity distribution functions
ℓ	= distance of panel apex from origin
m	= panel edge slope
M	= Mach number
r,θ	= angular coordinates
u,v,w	= perturbation velocities
x,y,z	= Cartesian coordinates
α	= angle of attack
β	= Prandtl-Glauert number = $(M^2-1)^{1/2}$
δ	= panel inclination angle

Introduction

SIGNIFICANT advances have recently been made in the application of surface singularity techniques to the analysis and design of complex aircraft configurations in subsonic and supersonic flow.[1-3] This has been accomplished by applying high-order source and doublet singularities on exact surface paneling, and by improved formulation of the boundary conditions. The application of surface panel techniques to the analysis of supersonic flows, however, has led to some unique numerical stability problems resulting in an undesirable sensitivity of the surface pressure to the panel subdivision and location of control points.

Basically, the problem arises when adjacent panels having discontinuities in slope produce waves in the interior flow, which reflect from the singularity sheets representing the opposite side of the configuration surface. Repeated reflections of these waves build up and affect the strength of the surface singularity distribution, which, in turn, introduces spurious perturbations in the exterior flow. Previous investigators[1,2] have attempted to eliminate the interior wave propagation by using a combination of source and doublet singularities, together with both interior and exterior boundary conditions. This technique has shown significant improvement over earlier attempts to solve this problem.

An alternate approach, described in this paper, is based on a new supersonic triplet singularity which eliminates the spurious internal waves generated by panels having supersonic edges. In particular, perturbation velocities in the "two-dimensional" region associated with supersonic panel edges are exactly cancelled in the interior flow. As a result, only external tangency boundary conditions are required to determine the strengths of the triplet singularities, and the resulting pressure distributions are free from the influence of spurious internal wave reflections.

Aerodynamic Theory

The triplet singularity is a linear combination of source and vortex singularity distributions. Since the vortex (or doublet) sheet may be considered the result of combining, in a special limiting process, two source sheets of equal and opposite strength, the combination of a vortex sheet of unit strength with a source sheet of strength β has been termed a triplet. A simple illustration of the basic concept for two-dimensional flow is given on Fig. 1. In this example, the axial and normal velocity component vectors add in the flowfield above the panel, but cancel exactly below the panel, resulting in the desired unidirectional perturbation velocity field.

The extension of this concept to the analysis of bodies having arbitrary cross section requires the derivation of three special triplet distributions.

Axial Triplet

The elementary source and vortex filaments making up an axial triplet distribution lie in the plane of the panel parallel to the x axis, as shown in Fig. 2a. The panel has unswept leading and trailing edges, but the side edges may have arbitrary sweep, m_1 and m_2. The side edges extended intersect the x axis at a distance ℓ from the origin.

The perturbation velocities at a point (x,y,z) in the field are obtained by integrating the contributions of the elementary source or vortex filaments across the panel in the y direction, using the method outlined in Ref. 3. The triplet perturbation

Presented as Paper 79-0273 at the AIAA 17th Aerospace Sciences Meeting, New Orleans, La., Jan. 15-17, 1979; submitted Feb. 15, 1979; revision received July 23, 1979. This paper is declared a work of the U.S. Government and therefore is in the public domain. Reprints of this article may be ordered from AIAA Special Publications, 1290 Avenue of the Americas, New York, N.Y. 10019. Order by Article No. at top of page. Member price $2.00 each, nonmember, $3.00 each. **Remittance must accompany order.**

Index categories: Aerodynamics; Supersonic and Hypersonic Flow; Analytical and Numerical Methods.

*Vice President. Member AIAA.

†Aerospace Technologist, Supersonic Aerodynamics Branch. Associate Fellow AIAA.

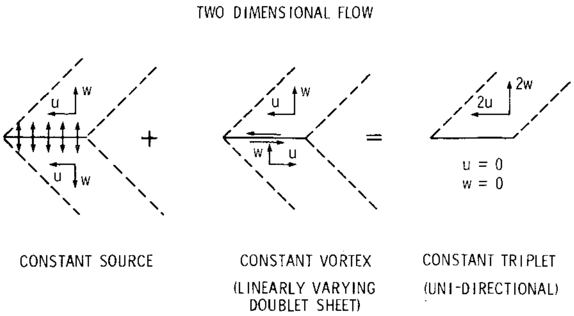

Fig. 1 Supersonic triplet concept.

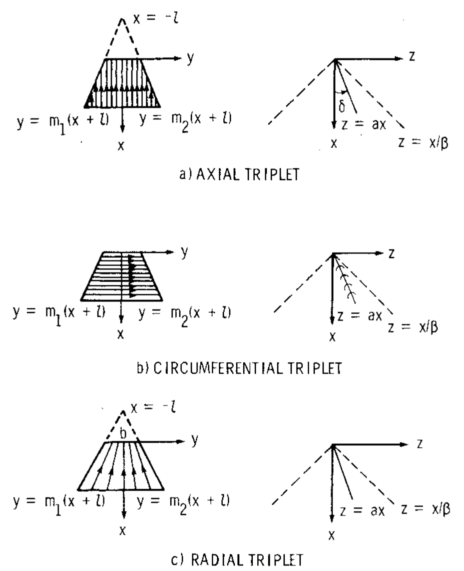

Fig. 2 Elementary triplet distributions.

velocities are then obtained by combining the source and vortex distributions in the manner described in the previous paragraph. Finally, the panel is rotated through the angle δ about the leading edge, using a Lorentz transformation, to obtain the three components of velocity associated with one corner of the panel.

$$u_A = d/[\beta(x-\beta z)] - aG \tag{1}$$

$$v_A = F+H \tag{2}$$

$$w_A = -\beta u_A \tag{3}$$

where

$$a=\tan\delta, \quad d=[x^2-\beta^2(y-m\ell)^2-\beta^2 z^2]^{1/2}$$

$$F=\tan^{-1}\frac{(z-ax)d}{x[m(x+\ell)-y]+\beta^2 z[ay-m(z+a\ell)]}$$

$$G=\log\frac{x+\beta^2[m(y-m\ell)+az]+[1-\beta^2(a^2+m^2)]^{1/2}d}{\beta\{[y-m(x+\ell)]^2-\beta^2[ay-m(z+a\ell)]^2+(z-ax)^2\}^{1/2}}$$

$$\times\frac{1}{[1-\beta^2(a^2+m^2)]^{1/2}}$$

$$H=\tan^{-1}\frac{d}{-\beta(y-m\ell)} \qquad \ell=\frac{b}{m_2-m_1}$$

The influence of the complete panel is obtained by summing the contributions of the four corners.

Circumferential Triplet

The elementary source and vortex filaments making up a circumferential triplet distribution lie in the plane of the panel parallel to the y axis, as shown in Fig. 2b. The details of the derivation of the three components of velocity for this source distribution are given in Ref. 3. The derivation for the votex distribution is similar. The triplet perturbation velocities in the field are obtained by combining the source and vortex velocity components as previously described, giving

$$u_c=\frac{F+H-\beta mG}{\beta(1-\beta a)} \tag{4}$$

$$v_c=G \tag{5}$$

$$w_c=-\beta u_c \tag{6}$$

Radial Triplet

The elementary source and vortex filaments making up the radial triplet distribution lie in the plane of the panel along radial lines from the intersection of the two side edges extended and the x axis, as shown in Fig. 2c. In this case, the perturbation velocities at a point in the field are obtained by integrating between the panel side edges with respect to the variable m. The resulting expressions are considerably more complex than the preceding two distributions, but simplify considerably when combined into triplet form, as follows:

$$u_R=\frac{C}{\beta}\left[\frac{\beta y[F+H-\beta yG_R]}{x+\ell-\beta(z+a\ell)}-\frac{d}{x-\beta z}+\beta(z+a\ell)G_R\right] \tag{7}$$

$$v_R=C(F+H-\beta yG_R) \tag{8}$$

$$w_R=C\left[\frac{\beta yF+H-\beta yG_R}{x+\ell-\beta(z+a\ell)}-\frac{d}{x-\beta z}+(x+\ell)G_R\right] \tag{9}$$

where

$$C=\frac{(1-\beta a)\ell}{x+\ell-\beta(z+a\ell)}$$

$$D=[(x+\ell)^2-\beta^2(y^2+z^2)]^{1/2}$$

$$G_R=1/D$$

$$\times\log\frac{x(x+\ell)-\beta^2 y(y-m\ell)-\beta^2 z(z+a\ell)+dD}{\beta|\ell|\{[y-m(x+\ell)]^2-\beta^2[ay-m(z+a\ell)]^2+(z-ax)^2\}^{1/2}}$$

It should be noted that the velocity distribution functions F and H always appear as a sum in the above triplet velocity formulas. This special relationship provides the desired internal wave cancellation in the two-dimensional region associated with the panel leading edge, since $F=\pi$ in the external flowfield, $F=-\pi$ in the interior flowfield, while $H=\pi$ in both the interior and exterior flow.

Application

A panel arrangement suitable for the analysis of a body having arbitrary cross section is shown in Fig. 3. The panel leading and trailing edges are defined by planes perpendicular to the reference axis, while the panel side edges are defined by continuous meridian lines. A grouping of six panels is required to make up a triplet singularity which will satisfy the Helmholtz vortex conservation laws without requiring discrete-edge vorticity or trailing-vortex wakes. Within this six-panel group, the individual singularity strengths are prescribed such that the elementary vortex filaments form closed loops, as indicated on the figure. The center row of panels contains only circumferential triplet singularities of

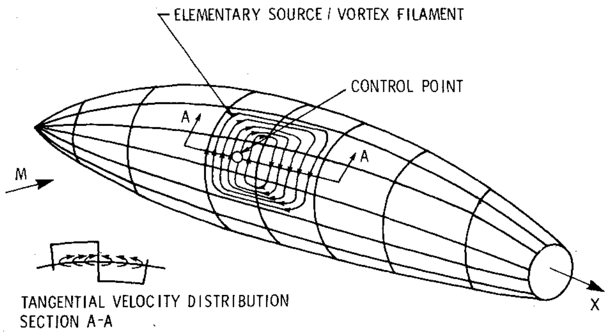

Fig. 3 Triplet panel grouping on arbitrary body at incidence.

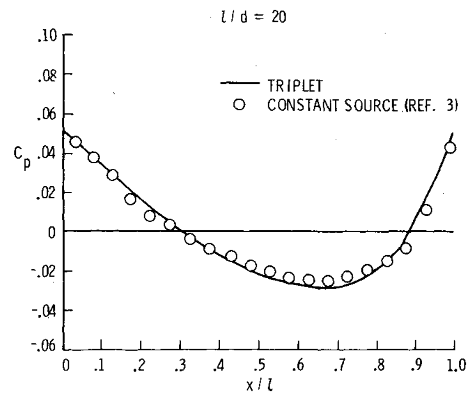

Fig. 4 Parabolic body; $M=\sqrt{2}$, $\alpha=0$ deg.

equal and opposite strengths. The singularities in the outer rows are composed of special combinations of all three basic types, which result in zero vorticity along the outer two edges, and match the inflow (or outflow) of vorticity along the inner two edges. This is achieved by summing the influence of the axial triplet and βm times the influence of the circumferential triplet, and subtracting the influence of the radial triplet.

One control point is associated with each panel group. The boundary condition of tangential flow is imposed at each of these control points, and the resulting system of linear equations solved to determine the individual triplet strengths. The surface pressure, forces, and moments acting on the body can then be calculated, based on the exact isentropic pressure coefficient formula. A computer code has been developed to perform the calculations and is available as a modification to the existing USSAERO program.[3]

Results and Discussion

Several examples are presented to illustrate the application of the triplet singularity method to a variety of body shapes in supersonic flow. The results are compared with other theoretical methods or experimental data.

Parabolic Body of Revolution

Figures 4 and 5 give the axial pressure distribution on a parabolic body of revolution having a fineness ratio of 20 at $M=\sqrt{2}$. Comparisons between the triplet method and the surface source method of Ref. 3 are shown for $\alpha=0$ and 5 deg. For this smooth slender body, the two methods give very similar results, although a close examination shows small irregularities in the pressure distribution calculated by the source method caused by internal wave reflections.

Cone-Cylinder-Cone

A more severe test case was provided by a 15 deg cone-cylinder-cone body at $M=2.0$. In this example, the surface source panel method of Ref. 3 fails to give a convergent solution. Figures 6 and 7 show the axial pressure distribution

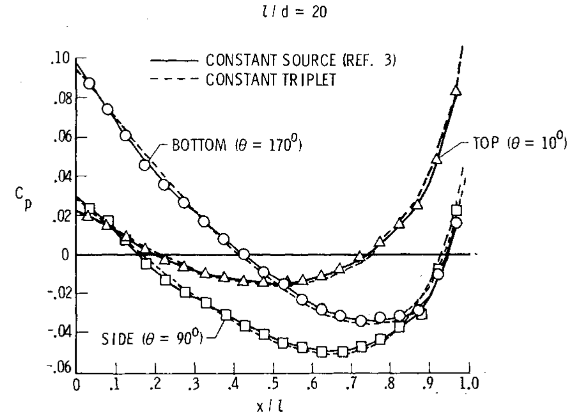

Fig. 5 Parabolic body; $M=\sqrt{2}$, $\alpha=5$ deg.

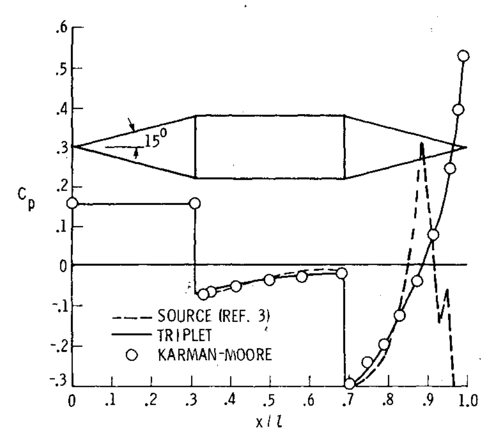

Fig. 6 15 deg cone-cylinder-cone; $M=2.0$, $\alpha=0$ deg.

at $\alpha=0$ and 10 deg, respectively, compared to that obtained by the classical Karman-Moore method.[4] (The Karman-Moore method uses a distribution of line sources and doublets along the axis, together with tangency boundary conditions on the body surface.) The results of these two methods agree closely, indicating that the triplet method has effectively eliminated the strong internal waves that caused the source method to diverge. Figure 8 shows the circumferential pressure distribution on the 15 deg cone at $M=2.0$ and $\alpha=10$ deg, on a section just behind the shoulder of the cone-cylinder and on a section of the cylinder extended 35 diameters behind the shoulder. The pressure distribution on this last section is seen to approach the incompressible crossflow on a circular cylinder in two dimensions.

Nacelle with Internal Flow

The exterior pressure distribution on a circular nacelle with internal flow has been calculated at $M=\sqrt{2}$ for $\alpha=0$ and 10 deg. The results are presented on Fig. 9. This example again indicates the effectiveness of the triplet singularity in suppressing spurious internal waves, and can be compared with the nacelle results presented in Ref. 2.

Ogive-Cylinder-Boattail

Figures 10 and 11 give the axial pressure distribution on an ogive-cylinder-boattail body at $M=2.3$. For $\alpha=0$ deg, Fig. 10, a comparison is made between the triplet method and the experimental data of Ref. 5. The theory tends to underestimate the pressure on the nose of the body, but agrees well with the data elsewhere, except on the boattail where viscous effects dominate. The underestimation of the nose pressure is a result of applying the linearized potential flow equations and tangency boundary conditions. A better approximation to the pressure on the nose can be obtained by

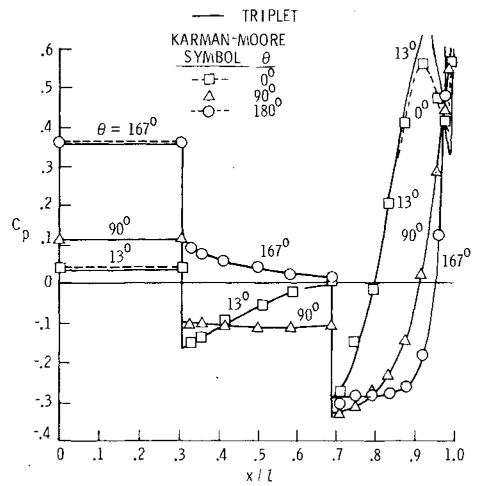

Fig. 7 15 deg cone-cylinder-cone; $M = 2.0$, $\alpha = 10$ deg.

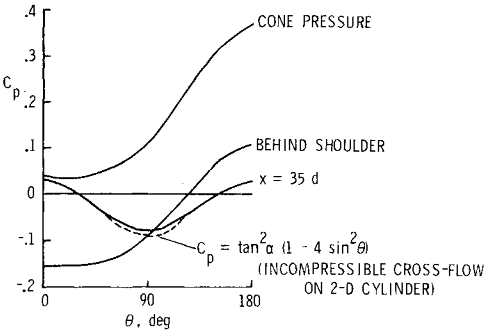

Fig. 8 Circumferential pressure distribution on 15 deg cone-cylinder; $M = 2.0$, $\alpha = 10$ deg.

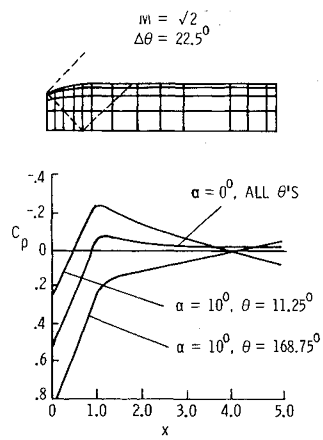

Fig. 9 Pressure distribution on nacelle; $M = \sqrt{2}$.

applying a correction based on the local Mach number obtained from the linearized solution. The improvement is indicated by the dashed line on the figure.

For $\alpha = 4$ deg, Fig. 11, a comparison is made among the triplet method, the finite-difference method,[6] and experimental data. The finite-difference method agrees well with the experimental data except on the boattail, while the triplet method again underestimates the pressure on the nose. No local Mach number correction has been added to the triplet results in this case.

Elliptic Cone

The triplet singularity may also be applied to the analysis of noncircular bodies. In Fig. 12, the circumferential pressure

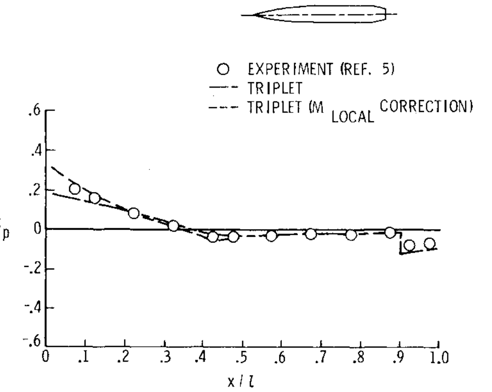

Fig. 10 Ogive-cylinder-boattail; $M = 2.3$, $\alpha = 0$ deg.

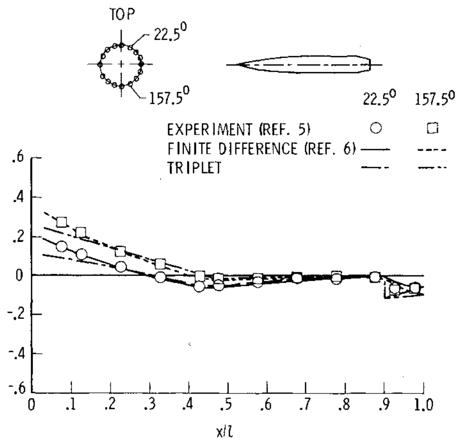

Fig. 11 Ogive-cylinder-boattail; $M = 2.3$, $\alpha = 4$ deg.

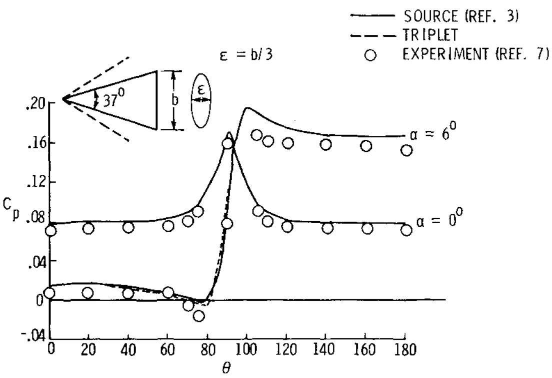

Fig. 12 Elliptic cone; $M = 1.89$.

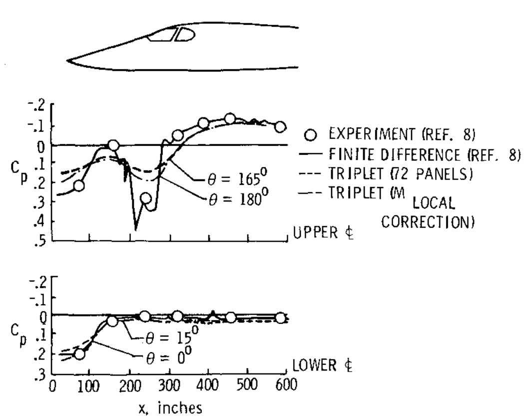

Fig. 13 B-1 forebody; $M = 2.2$, $\alpha = 3$ deg.

distribution on an elliptic cone at $M = 1.89$ is compared with experimental data.[7] For $\alpha = 0$ deg, the theory overestimates the pressure slightly. For $\alpha = 6$ deg, a more pronounced overestimation occurs on the lower surface.

B-1 Forebody

The pressure distributions along the upper and lower meridians of the B-1 forebody for $M = 2.2$ and $\alpha = 3$ deg are shown on Fig. 13. Results from the triplet method are compared with the finite-difference method and experimental data obtained from Ref. 8. The finite-difference method agrees exceptionally well with the experimental data in this example. On the other hand, the triplet method underestimates the pressure on the nose cone, and fails to predict the pressure peak behind the canopy shock. This result is due to the shortcomings of linearized potential flow theory and can be partially offset by applying a local Mach number correction to the theory.

Conclusion

A new triplet singularity distribution has been developed and applied to the aerodynamic analysis of a variety of body shapes in supersonic flow. The results appear to be insensitive to body paneling and compare favorably with those obtained by other linearized supersonic panel methods.

Acknowledgment

This research was supported by the NASA-Langley Research Center under Contract NAS1-12900.

References

[1] Ehlers, F. E., Johnson, F. T., and Rubbert, P. E., "A Higher-Order Panel Method for Linearized Supersonic Flow," AIAA Paper 76-381, July 1976.

[2] Ehlers, F. E., Epton, M. A., Johnson, F. T., Magnus, A. E., and Rubbert, P. E., "An Improved Higher-Order Panel Method for Linearized Supersonic Flow," AIAA Paper 78-15, Jan. 1978.

[3] Woodward, F. A., "An Improved Method for the Aerodynamic Analysis of Wing-Body-Tail Configurations in Subsonic and Supersonic Flow," NASA CR-2228, May 1973.

[4] von Kármán, T. and Moore, N. B., "The Resistance of Slender Bodies Moving with Supersonic Velocities with Special Reference to Projectiles," *Transactions of ASME*, Vol. 54, 1932, pp. 303-310.

[5] Landrum, E. J., "Wind Tunnel Pressure Data at Mach Numbers from 1.6 to 4.63 for a Series of Bodies of Revolution at Angles of Attack from −4° to 60°," NASA TM X-3558, Oct. 1977.

[6] Marconi, F., Salis, M., and Yaeger, L., "Development of a Computer Code for Calculating the Steady Super/Hypersonic Inviscid Flow Around Real Configurations," NASA CR-2675, Vol. 1: Computational Technique.

[7] Maslen, S. H., "Pressure Distribution on a Thin Conical Body of Elliptic Cross Section at Mach Number 1.89," NACA TN-2235, 1950.

[8] d'Attore, L., Bilyk, M. A., and Sergeant, R. J., "Three-Dimensional Supersonic Flow Field Analysis of the B-1 Airplane by a Finite-Difference Technique and Comparison with Experimental Data," AIAA Paper 74-189, Feb. 1974.